Spatio-temporally-complex concentration profiles using a tunable chaotic micromixer

Chia-Hsien Hsu
Department of Mechanical Engineering, University of Washington, Seattle, Washington 98195

Albert Folch[a)]
Department of Bioengineering, University of Washington, Seattle, Washington 98195

(Received 29 June 2006; accepted 1 August 2006; published online 4 October 2006)

The ability to present cells with stimuli that vary in space and time is key for a mechanistic understanding of dynamic processes such as cell migration, growth, adaptation, and differentiation. Microfluidic gradient devices that output multiple concentrations of a given compound exist, but changing the output generally requires a change in flow rates that can be confounding in biological measurements and/or impractical for high-throughput applications. We present chaotic mixers that generate multiple, complex concentration gradients that can be smoothly varied in time without significantly altering the flow rate. © *2006 American Institute of Physics*.
[DOI: 10.1063/1.2358194]

Cell-based bioassays consist of measuring cellular responses to a compound or set of compounds, usually before and after the compounds are added to the cell culture medium. Multi-well plates and robotic pipetters allow for combinatorial testing of compound mixtures or titrations prepared ahead of time, an approach that is becoming increasingly impractical as bioassay complexity increases with new genomic and proteomic data. Furthermore, these traditional cell culture substrates do not allow for testing the response of cells to biochemical gradients. The ability to change gradients in time is of great interest in biology because time is a central parameter in many gradient-directed cellular processes (such as cell chemotaxis, differentiation, and growth, via, e.g., desensitization and/or sequential gene activation) as well as in other processes not directed by gradients (such as adaptation to drugs or chemokines).

Microfluidic technology offers the possibility of integrating fluid switching and gradient generators with cell culture chambers in parallel operation,[1–15] thereby reducing reagent consumption, increasing portability and throughput, and enabling focal or graded stimulation compared to traditional Petri-dish or multi-well cell cultures. Continuous fluid flow over the cells is imperative to prevent diffusive broadening of the stimulus in applications such as requiring gradient formation,[3,13] focal stimulation,[2,14] or fast fluid switching.[11,15] Since those microfluidic devices have static architectures, changing the concentration profile inevitably requires changing the flow rate or the inlet connections, e.g., by manipulating the driving pressures or displacement pumps outside of the device or by activating microvalves and/or micropumps inside of the device. However, in cell-based experiments, the flow rate determines other biophysical parameters that strongly influence cell function, such as shear forces[16–18] and mass transport of necessary soluble species[19] (from nutrients and metabolites to gases), so a flow rate change can confound the measurements; for example, neutrophil migration can be biased towards downstream when placed in microfluidic chemotactic gradients.[20] Importantly, existing gradient generators can only create monotonic gradients between each pair of inlets[13] (one additional inlet is required for each maximum or minimum in the gradient profile,[3]) so complex gradients require correspondingly numerous inlets. (Several general-use combinatorial micromixers have been developed to produce static titrations or mixtures of compounds in continuous flow;[21–28] two constant-flow on/off micromixer designs exist; one, based on manually assembled miniature turbines, is not amenable to parallel fabrication;[29] the other one, based on transverse electroosmotic flow, requires electrical fields that are potentially adverse to cells.[30])

Here we present microfluidic "stirrers" (μFS) that (a) do not *require* flow rate changes to adjust mixing, and (b) can generate complex (nonmonotonic) concentration profiles (albeit not *arbitrarily* complex). As shown schematically in Figs. 1(a) and 1(b), the μFS is made by aligning/bonding three layers that are micromolded in poly(dimethyl siloxane) (PDMS): the top layer forms the flow-carrying microchannel and the bottom layer forms a set of grooves addressed by a pneumatic line, with a spin-cast thin PDMS membrane ($\sim$10 μm thick) sandwiched in between as described elsewhere.[31] The grooves are inactive when the pneumatic line is not pressurized [Fig. 1(a)]. With suction applied to the pneumatic line, the PDMS membrane deflects downward and the grooves "appear," inducing chaotic mixing[32] [Fig. 1(b)]. Stroock *et al.*[32] and others[33] have shown that (static) micrograooves induce a transverse momentum in the flow, thus creating a "helical" re-circulation (the laminar-flow equivalent of "stirring") that enhances mixing; the design is interesting because the channel length required for full mixing increases only logarithmically with flow rate (as opposed to proportionally for a smooth-wall microchannel). The amount of mixing depends on the design layout (a "striped" pattern is less efficient than a "herringbone" pattern) and increases with the depth of the grooves, but the presence of the grooves does not have a significant effect on the fluid flow resistance.[32] In our μFS, the depth of the grooves can be tuned but are otherwise of similar dimensions. If needed, the depth of the grooves can be measured by filling the channel or the pneumatic line with fluorescein (see below) and com-

[a)]Author to whom correspondence should be addressed; electronic mail: afolch@u.washington.edu

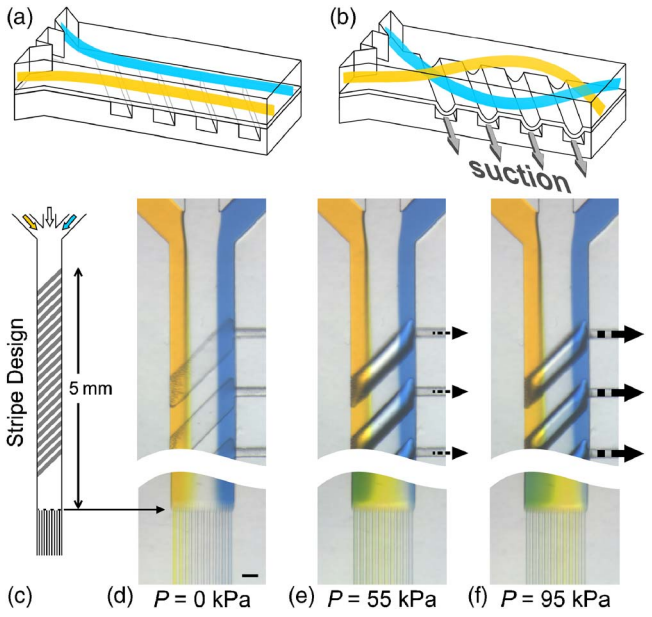

FIG. 1. (Color online) Operation of the μFS. (a) Flow in the microchannel is not stirred when the PDMS membranes are not pressurized; flow is from left to right. (b) Flow is stirred when suction is applied to the pneumatic line, deflecting the membrane downwards (deflection depending on P), which forms grooves. (c) Schematic diagram of the μFS (with stripes at 45° angle, 100 μm wide, 50 μm deep and 100 μm separation). (d)–(f) Optical micrographs illustrating temporal sequences of concentration gradients of yellow dye, water, and blue dye generated by the μFS (the microchannel is 200 μm wide and 80 μm tall; the outlet channels are 10 μm wide and 20 μm tall) when P=0 kPa (d), 55 kPa (e), and 95 kPa (f) is applied to the pneumatic channel; flow is from top to bottom. Scale bar=50 μm.

paring the fluorescence signal over and away from the grooves[31] (at P=100 kPa, the deflection is ~22 μm;for this membrane geometry the deflection at the apex is linear with applied pressure.[34])

The device contains a "stripe design" of grooves (45° angle, 100 μm width, 50 μm max. depth, and 100 μm separation) in a 35-mm-long microchannel (200 μm wide, 80 μm high) that ends in multiple outputs (each 10 μm wide, 20 μm high) [Fig. 1(c)]. The outlet channels serve the purpose of "sampling" the concentration distribution of the main channel at ten different points, which effectively creates a different titration in each channel (a "gradient"). With a three-inlet channel, the μFS can be used to produce (and change) combinations of compounds, as illustrated in Figs. 1(d)–1(f) (P=0, 55 and 95 kPa, respectively) with the mixing of three streams of blue and yellow dyes and water. Note that this device can be considered a gradient generator if the output channels were merged into one, as is usually done in other gradient generators.[26,28] The change in flow resistance due to changes in deflection is a small fraction of the total flow resistance of the whole fluidic network, so the flow rates (but not the flow *patterns*) are virtually independent of the depth of the grooves, in agreement with Stroock *et al.*[32] Similar effects can be achieved with a "herringbone design" (see Ref. 35).

For quantitative measurements of concentration profiles, we introduce fluorescein and water in a two-inlet channel. Since the charge coupled device camera used for these studies (Hamamatsu Orca-ER, 12 bit cooled) is highly linear under nonsaturating conditions, the grayscale intensity of any pixel in the image (after background correction to compensate for stray light and inhomogeneities in illumination) is a linear function of the fluorescein concentration in the fluid volume sampled by the pixel. For the flow rates used in this study, the concentration profile at the end of the channel takes a few seconds to reach steady state even for fast jumps in P, a fundamental limitation imposed by the Taylor dispersion typical of Pouseuille flow[36] (in other words, to the fact that fluid flows slower close to the walls); however, the transition is smooth (see Ref. 35). To minimize the effect that the pressure driving the flow has on membrane deflection (i.e., no two grooves can be at the same exact pressure differential), the pressure driving the flow must be set to be much smaller than the pressure applied to the membranes; in our device, even at P=0 the flow-induced residual deflection resulted in negligible stirring.

The μFS can generate complex concentration gradients that are difficult or impossible to create with other existing gradient generators. The fluorescence micrographs in Figs. 2(a)–2(c) show the three different concentration profiles generated with P=0, 60, and 85 kPa, respectively. Figure 2(d) shows a sequence of plots of the average fluorescence values in each output channel [obtained at the horizontal dashed line in Fig. 2(a)] for P=0–100 kPa, illustrating the range of complex shapes (from monotonic to two-maxima gradients, from decreasing to increasing slopes) that can be obtained with this design; further increases in P beyond ~100 kPa did not change the gradient appreciably. Note that the largest variations in shape occur at low P, suggesting that a better strategy to obtain a larger variety of shapes (work under way) would be to actuate different numbers of individually addressable grooves and/or use the more efficient herringbone design. Figure 2(e) is a different visualization of the same data used for Fig. 2(d) to emphasize the variety of temporal sequences of concentration values that can be obtained for any given output channel. The set of output concentrations generated by each actuation pressure is highly reproducible. Note that more complex sequences of actuation pressures could be used to generate more complex temporal sequences of concentration profiles (i.e., the pressures need not be increased or decreased monotonically).

In conclusion, we have demonstrated proof-of-principle microfluidic stirrers that allow for adjusting the degree of mixing at the outlet in real time by using depth-tunable grooves on the channel floor. The μFS has three salient features: (1) Complex, nonmonotonic gradients are possible with a simple two-inlet arrangement; (2) The gradients can be changed with time by changing P; at present, the variety of gradients that can be achieved is limited; and (3) changing the gradients does not significantly change the flow rates because the grooves do not cause a significant change in flow resistance. Given the chaotic nature of the flow patterns, the concentration profiles are likely to be a strong function of fabrication parameters (such as alignment, membrane thickness/stiffness, and channel dimensions–all of which are laboratory and/or expertise dependent) and of design layout, so a full characterization of the device is at present necessary prior to using the device for any given application. The present design is limited to ten outputs with all the (stripe) grooves activated simultaneously. Although the gradients cannot be generated with arbitrary complexity, in principle the design could contain many more outputs and grooves of various shapes could be activated in groups or individually to obtain a wider variety and finer control of the output concentration profiles. Such complex gradients should allow for

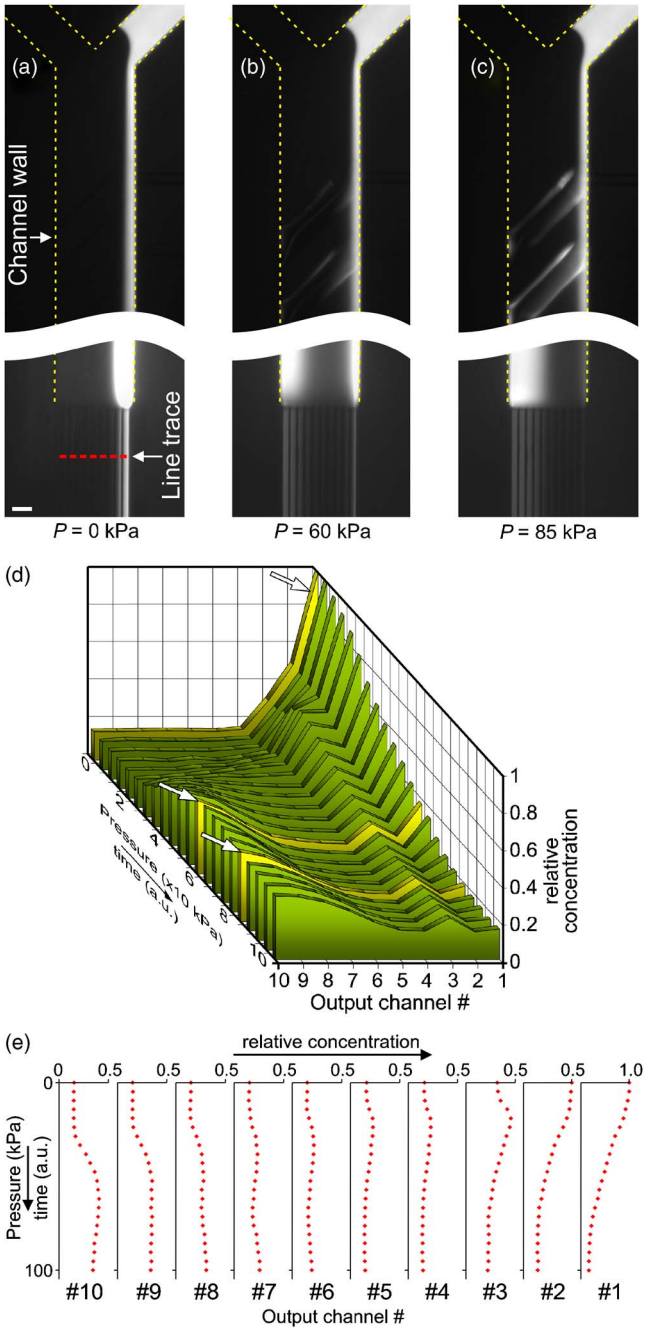

FIG. 2. (Color online) Parallel generation of multiple time-variable concentrations of fluorescein with the μFS. (a)–(c) Fluorescence micrographs of the device for $P=0$ kPa (a), 60 kPa (b), and 85 kPa (c); flow is from top to bottom. Scale bar=50 μm. (d) Plots of relative concentration of fluorescein as a function of channel number (gradients) for the range $P=0-100$ kPa; the three gradients in (a) are highlighted with an arrow; the vertical shading has been added to emphasize differences in relative concentration. (e) Fluorescence intensity values in each of the ten outlet channels vs P (or time); the values are normalized to the $P=0$ kPa value.

probing the effects of nonlinear gradients on cell chemotaxis.[3,37]

Furthermore, the ability to change many output concentrations in parallel with simple inlet arrangements should find uses in applications where high throughput is critical, such as in systems biology, drug/toxicology screening, and biotechnology (e.g., for optimizing bioreactor and co-culture medium formulations with multiple growth factors).

A National Science Foundation Career Award (A.F.) supported this work.

[1]T. Thorsen, S. J. Maerkl, and S. R. Quake, Science **298**, 580 (2002).
[2]S. Takayama, E. Ostuni, P. LeDuc, K. Naruse, D. E. Ingber, and G. M. Whitesides, Chem. Biol. **10**, 123 (2003).
[3]N. L. Jeon, H. Baskaran, S. K. W. Dertinger, G. M. Whitesides, L. Van de Water, and M. Toner, Nat. Biotechnol. **20**, 826 (2002).
[4]A. Tourovskaia, X. Figueroa-Masot, and A. Folch, Lab Chip **5**, 14 (2005).
[5]C. Ionescu-Zanetti, R. M. Shaw, J. G. Seo, Y. N. Jan, L. Y. Jan, and L. P. Lee, Proc. Natl. Acad. Sci. U.S.A. **102**, 9112 (2005).
[6]E. M. Lucchetta, J. H. Lee, L. A. Fu, N. H. Patel, and R. F. Ismagilov, Nature (London) **434**, 1134 (2005).
[7]Y. Lin, M. C. Nguyen, S. J. Wang, S. Gross, and N. L. Jeon, FASEB J. **17**, A448 (2003).
[8]P. Sabounchi, C. Ionescu-Zanetti, R. Chen, M. Karandikar, J. Seo, and L. P. Lee, Appl. Phys. Lett. **88**, 183901 (2006).
[9]P. J. Lee, P. J. Hung, V. M. Rao, and L. P. Lee, Biotechnol. Bioeng. **94**, 5 (2006).
[10]D. Irimia and M. Toner, Lab Chip **6**, 345 (2006).
[11]D. Irimia, S. Y. Liu, W. G. Tharp, A. Samadani, M. Toner, and M. C. Poznansky, Lab Chip **6**, 191 (2006).
[12]A. M. Taylor, M. Blurton-Jones, S. W. Rhee, D. H. Cribbs, C. W. Cotman, and N. L. Jeon, Nat. Methods **2**, 599 (2005).
[13]D. Irimia, D. A. Geba, and M. Toner, Anal. Chem. **78**, 3472 (2006).
[14]A. Tourovskaia, T. F. Kosar, and A. Folch, Biophys. J. **90**, 2192 (2006).
[15]A. Sawano, S. Takayama, M. Matsuda, and A. Miyawaki, Dev. Cell **3**, 245 (2002).
[16]H. D. Huang, R. D. Kamm, and R. T. Lee, Am. J. Physiol.: Cell Physiol. **287**, C1 (2004).
[17]S. Li, N. F. Huang, and S. Hsu, J. Cell. Biochem. **96**, 1110 (2005).
[18]G. M. Riha, P. H. Lin, A. B. Lumsden, Q. Z. Yao, and C. Y. Chen, Ann. Biomed. Eng. **33**, 772 (2005).
[19]G. A. Ledezma, A. Folch, S. N. Bhatia, M. L. Yarmush, and M. Toner, J. Biomech. Eng. **121**, 58 (1999).
[20]G. M. Walker, J. Q. Sai, A. Richmond, M. Stremler, C. Y. Chung, and J. P. Wikswo, Lab Chip **5**, 611 (2005).
[21]R. F. Ismagilov, J. M. K. Ng, P. J. A. Kenis, and G. M. Whitesides, Anal. Chem. **73**, 5207 (2001).
[22]R. F. Ismagilov, D. Rosmarin, P. J. A. Kenis, D. T. Chiu, W. Zhang, H. A. Stone, and G. M. Whitesides, Anal. Chem. **73**, 4682 (2001).
[23]P. C. Wang, D. L. DeVoe, and C. S. Lee, Electrophoresis **22**, 3857 (2001).
[24]N. Schwesinger, H. Frank, and H. Wurmus, J. Micromech. Microeng. **6**, 99 (1996).
[25]F. G. Bessoth, A. J. deMello, and A. Manz, Anal. Commun. **36**, 213 (1999).
[26]S. K. W. Dertinger, D. T. Chiu, N. L. Jeon, and G. M. Whitesides, Anal. Chem. **73**, 1240 (2001).
[27]C. M. Neils, Z. Tyree, B. A. Finlayson, and A. Folch, Lab Chip **4**, 342 (2004).
[28]M. Yamada, T. Hirano, M. Yasuda, and M. Seki, Lab Chip **6**, 179 (2006).
[29]G. A. Mensing, T. M. Pearce, M. D. Graham, and D. J. Beebe, Philos. Trans. R. Soc. London, Ser. A **362**, 1059 (2004).
[30]N. Sasaki, T. Kitamori, and H.-B. Haeng-Boo Kim, Lab Chip **6**, 550 (2006).
[31]C.-H. Hsu and A. Folch, Appl. Phys. Lett. **86**, 023508 (2005).
[32]A. D. Stroock, S. K. W. Dertinger, A. Ajdari, I. Mezic, H. A. Stone, and G. M. Whitesides, Science **295**, 647 (2002).
[33]H. Sato, S. Ito, K. Tajima, N. Orimoto, and S. Shoji, Sens. Actuators, A **119**, 365 (2005).
[34]J. M. Hoffman, J. Shao, C.-H. Hsu, and A. Folch, Adv. Mater. (Weinheim, Ger.) **16**, 2201 (2004).
[35]See EPAPS Document No. E-APPLAB-89-219640 for a movie and figure. This document can be reached through a direct link in the online article's HTML reference section or via the EPAPS homepage (http://www.aip.org/pubservs/epaps.html).
[36]G. E. Karniadakis and A. Beskok, *Micro Flows*, 1st ed. (Springer, New York, 2002).
[37]S. J. Wang, W. Saadi, F. Lin, C. M. C. Nguyen, and N. L. Jeon, Exp. Cell Res. **300**, 180 (2004).